Supporting information for 'Near surface properties derived from Phobos transits with HP^3 RAD on InSight, Mars'

N. Mueller[1], S. Piqueux[2], M. Lemmon[3], J. Maki[2], R. D. Lorenz[4], M. Grott[1], T. Spohn[1,5], S.E. Smrekar[2], J. Knollenberg[1], T.L. Hudson[2], C. Krause[6], E. Millour[7], F. Forget[7], M. Golombek[2], A. Hagermann[8], N. Attree[9], M. Siegler[10], and W.B. Banerdt[2]

[1]Institute of Planetary Research, German Aerospace Center (DLR), Berlin, Germany

[2]Jet Propulsion Laboratory, California Institute of Technology, Pasadena, CA, USA

[3]Space Science Institute, College Station, TX, USA

[4]Johns Hopkins Applied Physics Laboratory, Laurel, MD, USA

[5]International Space Science Institute (ISSI), Bern, Switzerland

[6]Microgravity User Support Center, German Aerospace Center (DLR), Cologne, Germany

[7]Laboratoire de Météorologie Dynamique (LMD/IPSL), Sorbonne Université, Centre National de la Recherche Scientifique, École Polytechnique, École Normale Supérieure, Paris, France

[8]Luleå University of Technology, Space campus, Kiruna, Sweden

[9]Faculty of Natural Sciences, University of Stirling, Stirling, UK

[10]PSI, SMU Earth Science, Dallas, TX, USA.

March 10, 2021, 9:24pm

Contents of this file

1. Text S1
2. Figures S1 to S4

Introduction

This supporting information provides the details of the numerical model of 1D heat conduction to calculate the temperature response to the transits of Phobos as observed by the InSight HP^3 Radiometer in text S1. The supporting figures S1 to S4 are modified versions of the Figures 2-3 in the main article showing all of the observed transits in comparison.

Text S1. The numerical calculation is based on the finite difference scheme in the work of (Kieffer, 2013), but modified to solve the equations implicitly. The finite difference equation is:

$$\frac{T_i - T_i'}{t - t'} = -\frac{H_{i+.5} - H_{i-.5}}{B_i \rho_i C_i} \tag{1}$$

where T is temperature, i indicates the i^{th} layer, t is time, a prime indicates the previous time-step, $H_{i+.5}$ indicates the heat flow through the top of the i^{th} layer,$H_{i-.5}$ same through the bottom, B is layer thickness, ρ is density, and C is specific heat capacity.

The temperatures of the top and bottom of layer interface, $T_{i-.5}$ and $T_{i+.5}$ respectively, are:

$$T_{i-.5} = T_i + \frac{H_{i-.5} B_i}{2k_i} \tag{2}$$

$$T_{i+.5} = T_i - \frac{H_{i+.5} B_i}{2k_i} \tag{3}$$

Calculating this interface starting from the layer below and substituting for $T_{i+.5}$ provides the interface heat flow (same approach for top of layer interface):

$$H_{i+.5} = \frac{-2(T_{i+1} - T_i)}{B_i/k_i + B_{i+1}/k_{i+1}} \tag{4}$$

$$H_{i-.5} = \frac{-2(T_i - T_{i-1})}{B_i/k_i + B_{i-1}/k_{i-1}} \tag{5}$$

At the uppermost layer ($i = 1$) the heat flow through the upper interface (the surface) is the boundary condition:

$$H_{.5} = (1 - a)H_{\rm vis} + e(H_{\rm ir} - \sigma_b T_{.5}^4) \tag{6}$$

Here a is visible albedo, $H_{\rm vis}$ incident visible band heat flux e is infrared emissivity, $H_{\rm ir}$ is infrared incident heat flux, and σ_b is the Stefan-Boltzmann constant. The incident heat fluxes are calculated using the KRC model (Kieffer, 2013) with the atmospheric opacity derived from imaging of the sky. At the lower boundary condition at $i = N$ the geothermal heat flow is $H_{N+0.5} = H_{geo}$. The geothermal heat flow is here assumed to be zero, since within the range of plausible values it is not significant for the observable temperature.

The solution of the set of non-linear implicit equations 1 is found by iteratively approaching the set of $N + 2$ temperatures $[T_{.5}, T_1, T_2, T_3, ...T_N, T_{N+.5}]$ that are the root of the function:

$$F_i = -\frac{H_{i+.5} - H_{i-.5}}{B_i \rho_i C_i} - \frac{T_i - T_i'}{t - t'} \tag{7}$$

using Broyden's method (Press et al., 1992). To reduce number of calculations per step this equation is simplified to:

$$F_i = \frac{2(T_{i+1} - T_i)}{B_i \rho_i C_i (\frac{B_i}{k_i} + \frac{B_{i+1}}{k_{i+1}})} - \frac{2(T_i - T_{i-1})}{B_i \rho_i C_i (\frac{B_i}{k_i} + \frac{B_{i-1}}{k_{i-1}})} - \frac{T_i - T_i'}{t - t'} \tag{8}$$

In the special case of the bottom and top layer centers ($i = 1, i = N$) the finite difference is evaluated at the surface and bottom interface, so half a layer thickness and constant parameters are assumed for the heat flow calculation:

$$H_{N+.5} = -\frac{2k_N(T_{N+.5} - T_N)}{B_N} \tag{9}$$

$$H_{1-.5} = -\frac{2k_1(T_1 - T_{.5})}{B_1} \tag{10}$$

Thus Eq. 7 is for these special cases:

$$F_1 = \frac{2(T_2 - T_1)}{B_1\rho_1 C_1(B_1/k_1 + B_2/k_2)} - \frac{2k_1(T_1 - T_{.5})}{B_1^2\rho_1 C_1} - \frac{T_1 - T_1'}{t - t'} \tag{11}$$

$$F_N = \frac{2k_N(T_{N+.5} - T_N)}{B_N^2\rho_1 C_1} - \frac{2(T_N - T_{N-1})}{B_N\rho_N C_N(B_N/k_N + B_{N-1}/k_{N-1})} - \frac{T_N - T_N'}{t - t'} \tag{12}$$

Further we define $\Delta t = t - t'$ and $G_i = F_i\Delta t$ and the following coefficients that are calculated once per model time-step based on the previous temperature state:

$$f_i = \frac{2\Delta t}{B_i\rho_i C_i(B_i/k_i + B_{i+1}/k_{i+1})}, \text{for } i = 1, ...N-1 \tag{13}$$

$$f_N = \frac{2k_N\Delta t}{B_N^2\rho_1 C_1} \tag{14}$$

$$b_i = \frac{2\Delta t}{B_i\rho_i C_i(B_i/k_i + B_{i-1}/k_{i-1})}, \text{for } i = 2, ...N \tag{15}$$

$$b_1 = \frac{2k_1\Delta t}{B_1^2\rho_1 C_1} \tag{16}$$

With the notation for the sake of simplicity of implementation: $T_0 = T_{0.5}$ and $T_{N+1} = T_{N+0.5}$ the equation for root finding is then:

$$G_i = f_i(T_{i+1} - T_i) - b_i(T_i - T_{i-1}) - T_i + T_i' \text{, for } i = 1, ...N \tag{17}$$

The top and bottom temperatures T_0 and T_N+1 are determined by the heat flow boundary conditions:

$$G_0 = \frac{2k_1(T_1 - T_0)}{B_1} + (1-a)H_{\text{vis}} + e(H_{\text{ir}} - \sigma_b T_0^4) - h_{\text{conv}} T_0 \tag{18}$$

$$G_{N+1} = \frac{2k_N(T_{N+1} - T_N)}{B_N} + H_{geo} \tag{19}$$

Broyden's method iterates solutions to Eq. 17 and Eq. 18 to find of $N+2$ temperatures T_i for which G_i converges to zero.

References

Kieffer, H. H. (2013, March). Thermal model for analysis of Mars infrared mapping. *Journal of Geophysical Research (Planets)*, *118*(3), 451-470. doi: 10.1029/2012JE004164

Press, W., Teukolsky, S., Vetterling, W., & Flannery, B. (1992). *Numerical Recipes in C* (2nd ed.). Cambridge, UK: Cambridge University Press.

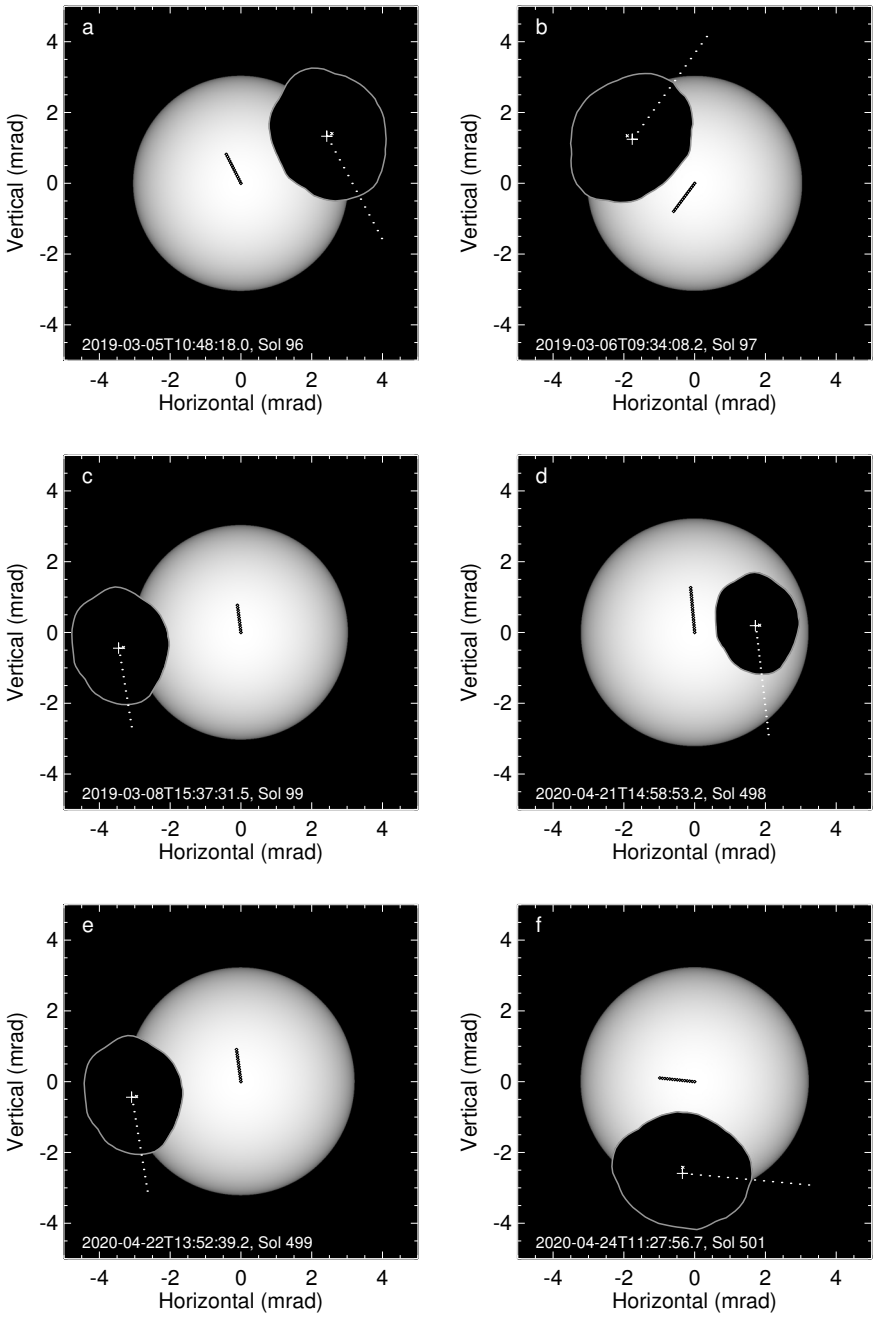

Figure S1. Simulated images of the moment of smallest angular separation of Phobos and Sun of all transits. The white + symbol indicates the Phobos Barycenter position, while the smaller x symbol indicates an offset of the Phobos barycenter for 1 km along the rotation axis towards the north pole.

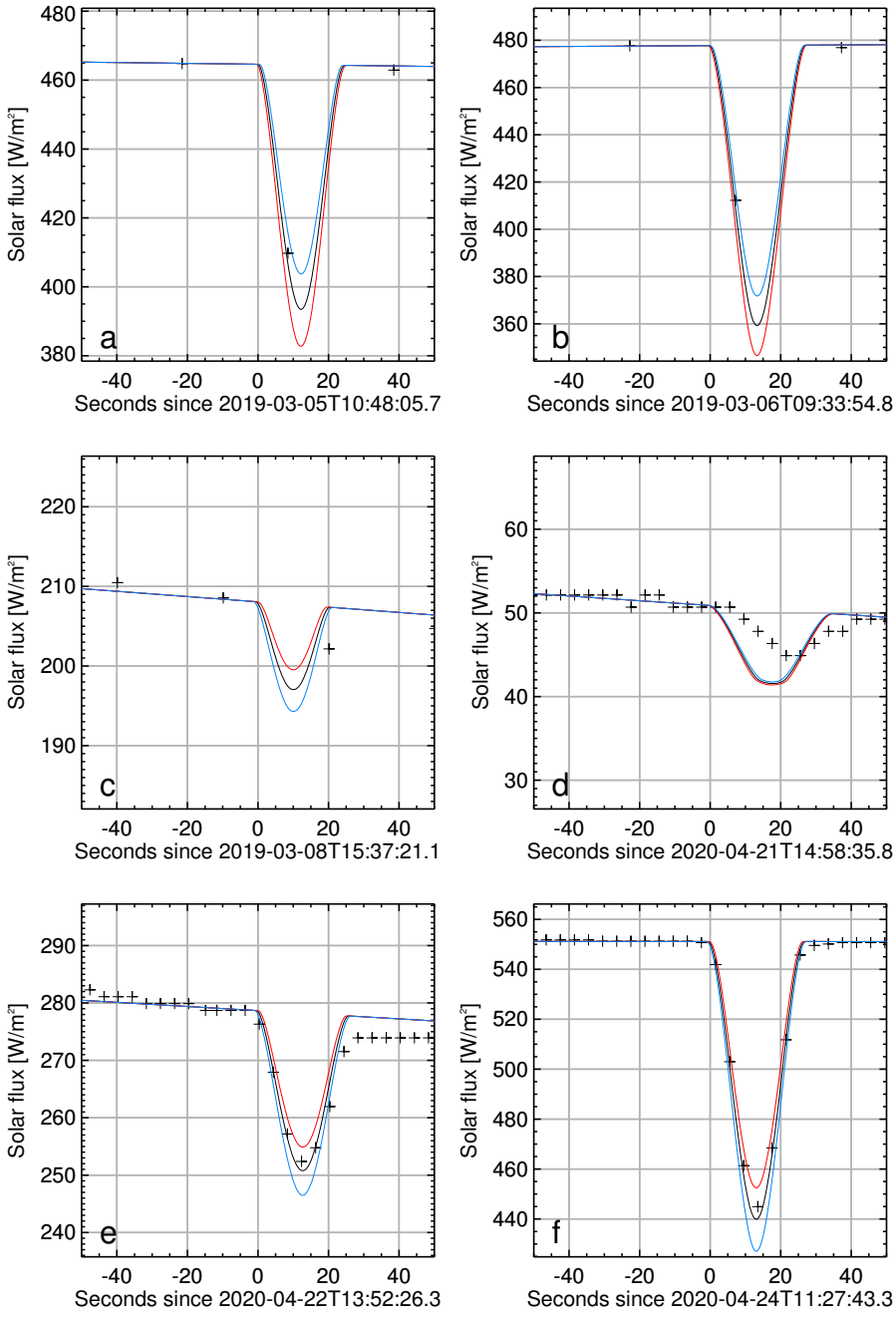

Figure S2. The simulated lightcurves in comparison to scaled solar panel currents for all transits. The symbols represent readings of the solar panel currents and the solid curves correspond to modeled lightcurves, where the blue and red curves correspond to position of Phobos that is ±1 km offset along its rotation axis.

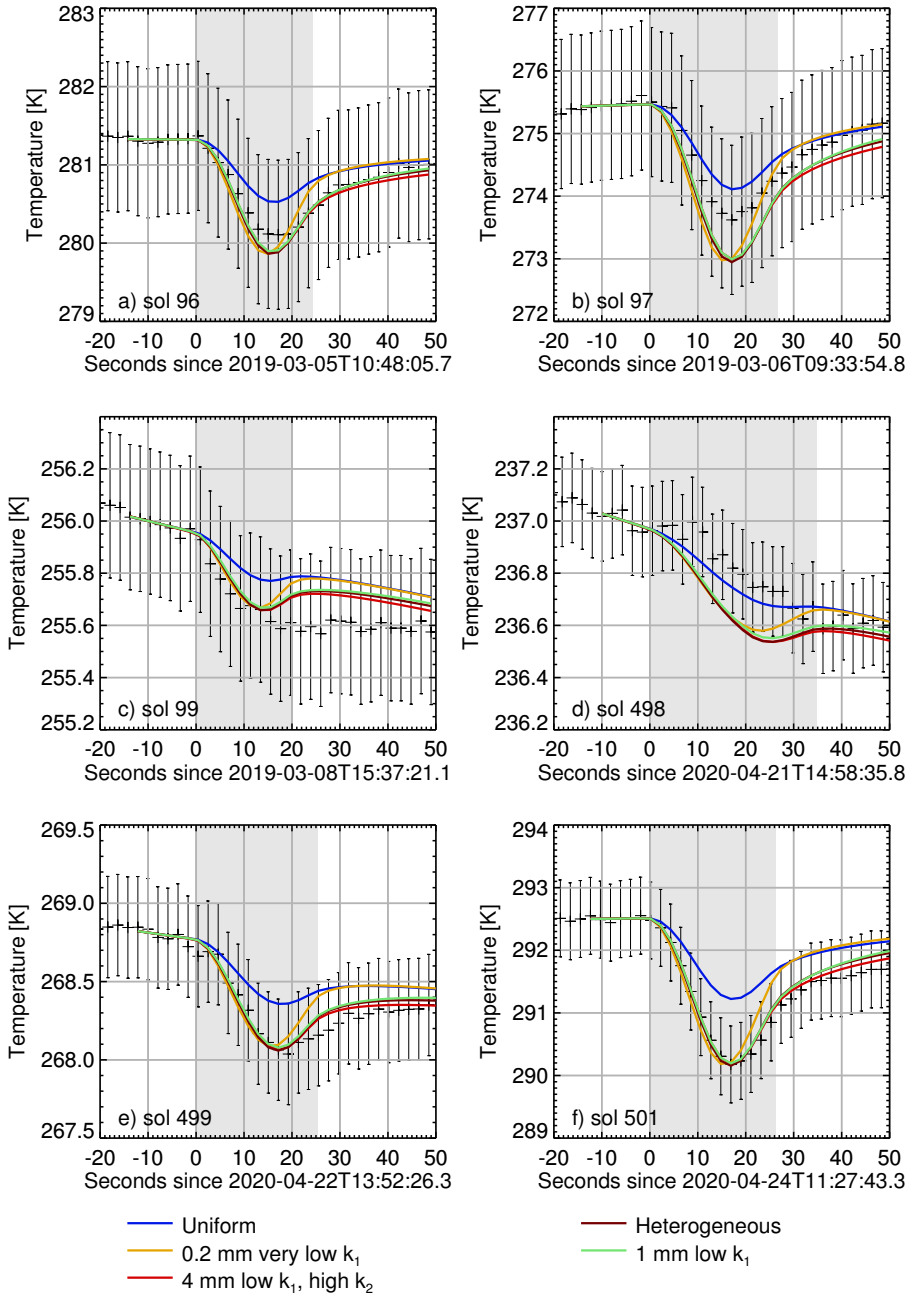

Figure S3. The temperature response of the surface during all transits observed by RAD together with several models for comparison. An offset is added to each model so that the data and model temperatures match on average in the 20 seconds preceding the transit. The model parameter details are described in the text of the main article.

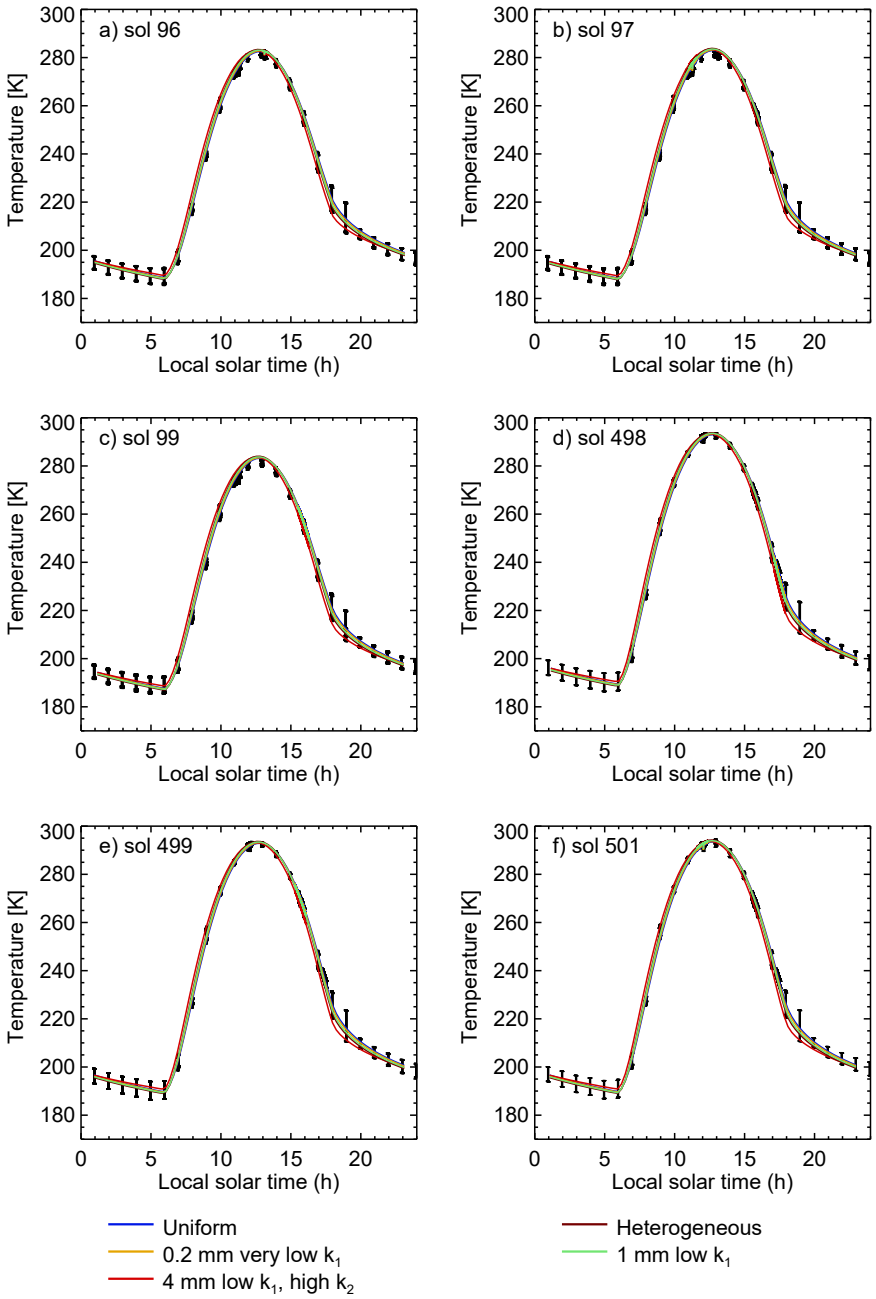

Figure S4. The diurnal surface temperatures observed within 3 sols of each transit. The error bars are total uncertainty of the radiometer which is mostly related to calibration uncertainty with only a minor contribution from atmospheric noise. Also plotted are the same models as described in the text of the main article.